Incorporating reflection data into refraction statics solution

Bernard K. Law, Daniel Trad*

ABSTRACT

Near surface models from refraction inversion contain several types of errors,which are partially compensated later in the data flow by reflection residual statics. In this work we modify the dataflow to automatically include feedback information from surface consistent reflection statics from stack-power maximization. We modify GLI by adding model and data weights computed from the long wavelength components of surface consistent residual statics. By using an iterative inversion, these weights allow us to update the near surface velocity model and to reject first arrival picks that do not fit the updated model. In this non-linear optimization workflow the refraction model is derived from maximizing the coherence of the reflection energy and minimizing the misfit between model arrival times and the recorded first arrival times. This approach can alleviate inherent limitations in shallow refraction data by using coherent reflection data.

INTRODUCTION

Refracted first arrivals from seismic reflection surveys are used to compute near surface velocity model for initial statics corrections for most land seismic data processing. Without this initial statics corrections, subsequent reflection velocity analysis and residual statics computation can be compromised. However, refraction statics corrections often contain data error,ε_d, numerical error,ε_m and algorithm error,ε_p, when the refraction algorithm is unable to model the actual physical properties of the near surface. This can result in unsatisfactory static and reflection images. These problems are often revealed on CDP stack sections, and are typically addressed by revising refraction algorithm parameters and constraints and by surface consistent residual statics using deeper reflection data.

Using a surface-consistent hypothesis Taner (1976) showed that correlation difference time between traces is the sum of shot, receiver, cdp and offset corrections. Ronen and Claerbout (1985) demonstrated that surface-consistent residual statics can be estimated by stack-power maximization. Eaton,Cary and Schafer (1991) modified stack-power maximization algorithm to optimize the running mix of the stack data. Henley (2012) presented an interferometric statics correction technique in radial trace domain for cases where surface consistency and stationarity are violated.

Statics estimation is effectively a velocity analysis of the near surface (Ronen and Claerbout, 1985); however, surface-consistent residual statics derived from more coherent and better sampled reflection data are not used in refraction inversion algorithms. In this paper, refraction inversion workflow utilizing residual statics solution to estimate the refraction data error, ε_d, model error,ε_m, and to improve near surface velocity model and refraction statics corrections will be discussed.

*CREWES

Near Surface Statics Correction

Normal moveout correction assumes straight rays between shot and reflector and between receiver and reflector (Figure 1); therefore time delays caused by near surface low velocity layers must be corrected before normal moveout velocity analysis and correction. For processing referenced from datum, datum statics correction is also required.

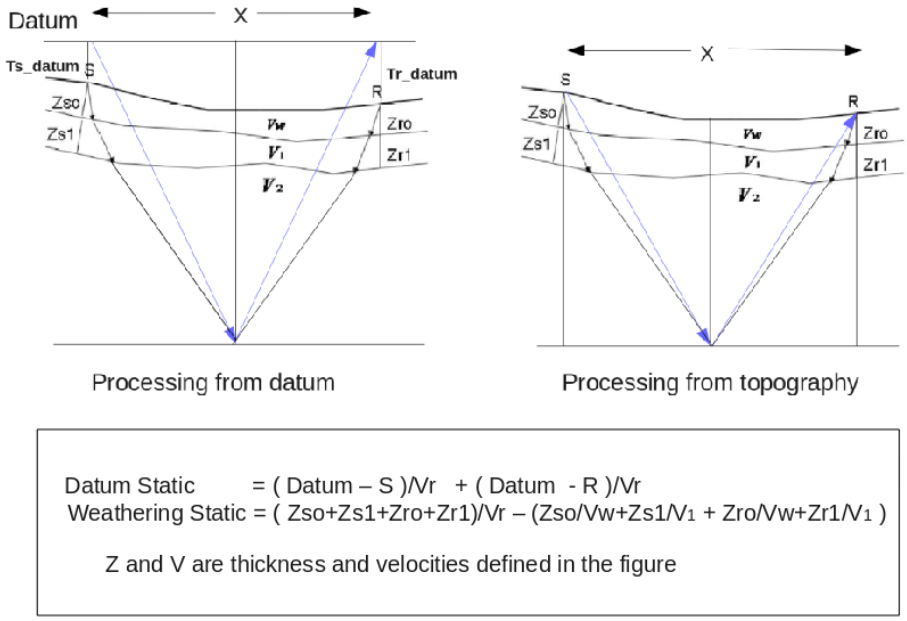

FIG. 1. Effect of surface elevation and low velocity layers on reflection time

Seismic Refraction

When a wave encounters abrupt change in the elastic properties parts of its energy is reflected and the remaining energy is refracted. The angle of reflection equals the incident angle and the angle of refraction is governed by the law of refraction, also known as the Snell's law (Figure 2). When V2 is greater than V1 and $\theta 2$ reaches 90° , the refracted ray will travel along the interface and will be refracted again up to the surface. The angle of incident for which $\theta 2$=90° is the critical angle (Figure 3).

Besides reflected and refracted energy, direct wave is also recorded by the receivers (Figure 4). For refraction analysis only first arrival times from direct wave and refracted wave are used.

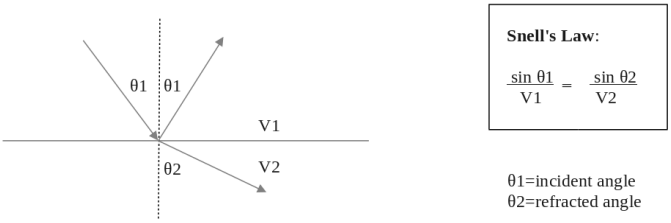

FIG. 2. Snell's Law

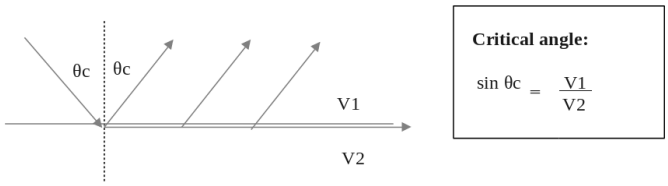

FIG. 3. Critical angle

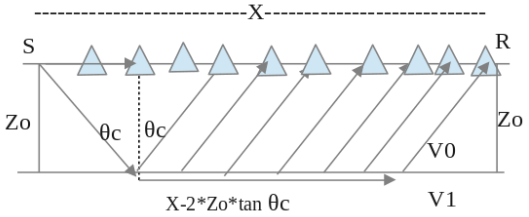

FIG. 4. Seismic Refraction

$$Travel\ time\ for\ direct\ wave = \frac{X}{V0} \tag{1}$$

$$Travel\ time\ for\ refracted\ wave = \frac{2 \times Zo}{V0 \times cos\theta c} + \frac{X}{V1} \tag{2}$$

where : $\cos\theta c = \sqrt{1 - sin\theta c \times sin\theta c} = \sqrt{1 - \frac{V0 \times V0}{V1 \times V1}}$

$\tan\theta c = \frac{sin\theta c}{cos\theta c}$

Delay Time Concept

The delay time concept was introduced by Gardner (1939) and further expanded by Barry(1967). Barry defined delay times δSB and δCR as raypath times between datum and refractor minus the time necessary to travel the normal projection of the raypath on the refractor (Figure 5). Delay time concept is used by many layer based refraction algorithms.

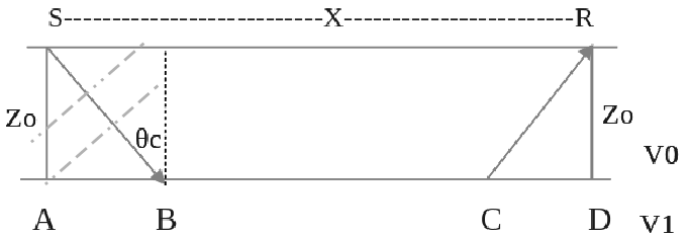

FIG. 5. Ray paths for delay time concept

$$\delta SB = \frac{SB}{V0} - \frac{AB}{V1}$$
$$\delta CR = \frac{CR}{V0} - \frac{CD}{V1}$$

With delay time concept, total travel time from S to R can be expressed as:

$$T = \delta SB + \delta CR + \frac{X}{V1} \tag{3}$$

Gardner (1939) showed that from the raypath geometry (Figure 5) and Snell's law:

$$\delta SB = \frac{Zo \times cos\theta c}{V0} \tag{4}$$

Assuming constant layer thickness, the refraction travel time can be represented by:

$$T = 2 \times \frac{Zo \times cos\theta c}{V0} + \frac{X}{V1} \tag{5}$$

On a T vs X display (Figure 6) delay time is represented by the intercept time at zero offset.

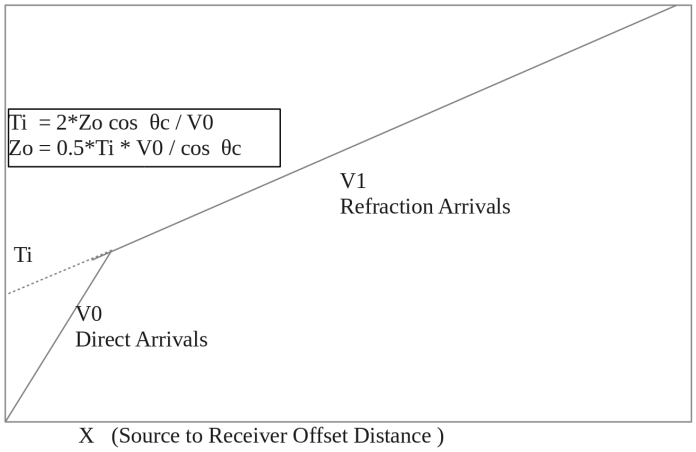

FIG. 6. TX Plot

Equation 5 can be written for the nth layer as:

$$T_k = \int_1^n 2 \times \frac{Z_k \times cos\theta c_k}{V_{k-1}} + \frac{X}{V_k} \tag{6}$$

Generalized Linear Inversion of layered refraction model

Hampson and Russell (1984) used the delay time equation to compute the model perturbation via first order Taylor expansion (Lines and Treitel 1984) and related the error in T to the model perturbation using the following set of linear equations.

$$\triangle T = B \triangle M \tag{7}$$

where : ΔT = change in ray traced time between iterations

B = ∂T_i / ∂m_i

$T_k = \int_{j=1}^{k} 2 \times Z_{k,j} \times cos\theta c \times P_{k-1,j} + X \times P_{k,j}$

i=observation number

j=surface station location or model parameter number

k=refractor number
ΔM = change in model parameter between iterations

The least square solution for ΔM is $(B^T B)^{-1} B^T \Delta T$

$$B = \frac{\partial T_i}{\partial m_i} \tag{8}$$

$$\frac{\partial T_i}{\partial p} = -2 Z_k tan\theta c + X_k \tag{9}$$

$$\frac{\partial T_i}{\partial z} = 2 cos\theta c \times P_{k-1} \tag{10}$$

Equation 9 is used to form the B matrix for the solution of ΔP and equation 10 is used to form the B matrix for the solution of ΔZ .

Common problems for refraction inversion

1. Insufficient sampling due to lack of long offset or physical surface obstacles:
   For tomographic inversion, it is important to understand the ray density or ray path redundancy within velocity cells by examining the ray density display to choose appropriate velocity grid size.

2. Poor quality first breaks caused by source, near surface coupling and noise problems:
   Interative editing and/or repicking of first breaks guided by updated refraction model or reflection constraints is a possible improvement.

3. Dispersion and attenuation of first arrival energy with offset.

4. Over-simplified assumptions used in refraction algorithms might not be adequate for some near surface condition.

These problems can result in the following three errors in refraction statics solution:
ε_d = data error
ε_m = numerical error in model parameters
ε_p = error in modeling the physics of the near surface

REFRACTION INVERSION UTILIZING STACK-POWER MAXIMIZATION

Model and Data Regularization

High-quality solutions to geophysical inverse problems require appropriate data and model regularization. In general, regularization in data space help to reduce the effect of outlying picks (Zhou,Gray,Young,Pham and Zhang 2003). Data weighting functions, W_d, and imaging weighting functions,W_m in the cost function are a commonly used approach in geophysics (Claerbout 1992). Following an approach similar to Trad et al.(2003) we build a cost function including W_d and W_m for the modified GLI algorithm.

$$J = ||W_d d - W_d L W_m m||^2 \tag{11}$$

Stack-power maximization

Ronen and Claerbout (1985) proposed a method to estimate surface-consistent residual statics by maximizing the stack power:

$$MAX(Power(m,d) - F(m)) \tag{12}$$

where: m is the shot and receiver statics
d is the CDP stack.
Power(m,d) is the sum of the stack-power of CDP stack traces for each combination of shot and receiver statics.
F(m) is the optional penalty function used for model constraint

Ronen and Claerbout's method iteratively maximizes the CDP stack power by aligning super-traces in shot and geophone domains with similar super-traces in CDP domain. Eaton and Cary (1991) developed a modified stacking power algorithm that uses the running-mix of the stacked data to form "super-duper" trace and modified the objective function to:

$$E' = \int_k \int_t [\int_{l=1}^{n} U_{k+l}(t)]^2 \tag{13}$$

where: E' is the total stacking power of the running-mixed stack
k is the CDP location
n is number of traces to sum

Surface-consistent residual statics estimated by stack-power maximization do not suffer the limitations of the first arrival data and refraction algorithms. We propose a method to incorporate these measurements in the estimation of W_m. Applying refraction statics computed from W_mm will yield the same stacking result as applying the surface-consistent residual statics. Using W_mm to iterate for a better near surface velocity model is similar to repicking NMO velocity model for migration instead of just applying residual moveout. The step of using W_mm to iterate to a better solution is not guaranteed to match the result from residual statics, because this process is again limited by the quality of refraction data and approximations of the refraction algorithms. However, this process will continuously improve the refraction model and first arrival picks by maximizing the stack-power.

Estimation of W_{mv} and W_{mz} by stack-power maximization

Surface consistent residual statics can be separated into long wavelength and short wavelength components. Long wavelength component is used to compute W_{mv} for velocity. For layer based method such as GLI it is also used to compute W_{mz} for thicknesses, and the values for W_{mv} and W_{mz} should be halved.

Computation of W_{mv} for velocity

We start with the weathering statics correction equation:

$$T_{i+1} = \frac{Z_{i+1}}{V_r} - Z_{i+1} \times P_1 \tag{14}$$

Adding reflection error E_i and W_{mvi} to equation 21 yields:

$$\begin{aligned} T_{i+1} + E_i &= \frac{Z_{i+1}}{Vr} - Z_{i+1} \times P_i \times W_{mvi} \\ Z_{i+1} \times P_i \times W_{mvi} &= \frac{Z_{i+1}}{V_r} - T_{i+1} - E_i \\ Z_{i+1} \times P_i \times W_{mvi} &= Z_{i+1} \times P_i - E_i \\ W_{mvi} &= 1 - \frac{E_i}{Z_{i+1} \times P_i} \end{aligned} \tag{15}$$

where: $E_i = E\frac{Z_{i+1}}{\int_{j=2}^{n} Z_j}$

E is the measured long wavelength reflection time error
Z_i is refractor layer thickness
E_i is reflection time error assigned to Z_i

Computation of W_{mz} for thickness

We start with the weathering statics correction equation:

$$T_{i+1} = \frac{Z_{i+1}}{V_r} - Z_{i+1} \times P_1 \tag{21}$$

Adding reflection error E_i and W_{mzi} to equation 21 yields:

$$\begin{aligned} T_{i+1} + E_i &= Z_{i+1}\frac{W_{mzi+1}}{Vr} - Z_{i+1} \times P_i \times W_{mzi+1} \\ Z_{i+1} \times P_i \times W_{mzi+1} - \frac{Z_{i+1} \times W_{mzi+1}}{V_r} &= -T_{i+1} - E_{zi} \\ W_{mzi+1} &= \frac{-T_{i+1} - E_{zi}}{Z_{i+1} \times P_i - \frac{Z_{i+1}}{V_r}} \\ W_{mzi+1} &= 1 + \frac{E_{zi}}{T_{i+1}} \end{aligned} \tag{16}$$

where: $E_i = E_z \frac{Z_{i+1}}{\int_{j=2}^{n} Z_j}$

E_z is the measured long wavelength reflection time error

Z_i is refractor layer thickness

Computation of W_d

Modeled first arrival times are computed using:

$$modeled\ arrival\ time = LW_m m \tag{17}$$

W_d is computed to reject first arrival picks that are more than **n** times the standard deviation of the residual errors. Residual error is computed by subtracting modeled first arrival time for the first arrival picks.

$$\delta T = d - LW_m m \tag{18}$$

$$Wd_i = \begin{cases} 0 & E_i >= \epsilon \text{ and } \delta\text{T} > \text{n} \times \text{std}(\delta\text{T}) \\ 1 & \text{otherwise} \end{cases}$$

where: E_i is the long wavelength reflection time error assigned to Z_i

δT is the difference between the picked and modeled first arrival time

ϵ is the error threshold for E_i below which Wd_i will be 1

std(δT) is the standard deviation of δT

n $\times$ std(δT) is the error threshold for δT below which Wd_i will be 1

Inversion workflow

1. Minimize J=|| d - Lm ||^2

Apply refraction statics (C_{wx} + ε_d + ε_m + ε_p)

C_{wx} = desired weathering correction

ε_d = data error

ε_m = numerical error in model parameters

ε_p = error in modeling physics of the near surface

2. Compute surface consistent residual static E using macro-binned stack-power maximization. Separate surface-consistent residual statics into long wavelength and short wavelength components

3. Compute W_m and W_d

4. If required, repick first arrival times using W_mm modeled first arrival times as constraints

5. Minimize J = || W_dd - W_dL W_mm ||^2

6. Iterate 2 to 5 until convergence criteria is met

7. Output improved weathering statics correction ($C_{wx} + \varepsilon_p$)

ε_p should be very small if the assumption of the refraction algorithm does not deviate too far from the actual physics of the near surface

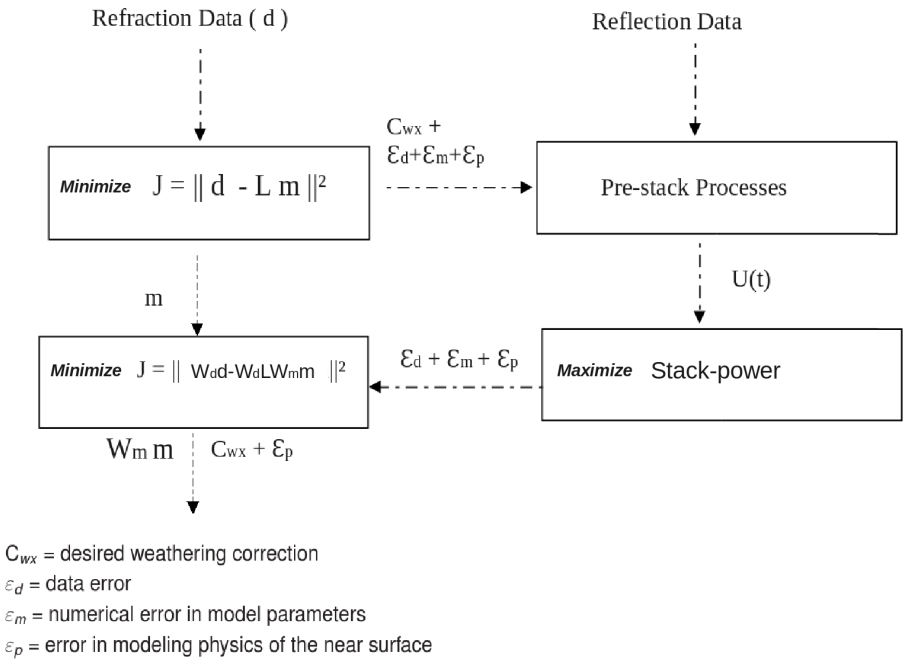

FIG. 7. Refraction inversion work flow utilizing feedback from reflection stack

GLI Refraction Analysis of Finite Difference Synthetic Dataset

To evaluate the GLI refraction solution software developed for this research, a synthetic dataset using 2^{nd} order finite-difference modeling was created using a velocity model with 6 layers of velocities 1000,2000,2500,3000,3500 and 4000 m/sec. Both receiver spacing and the depth step were 5 m. Figure 8 shows the near surface part of the model.

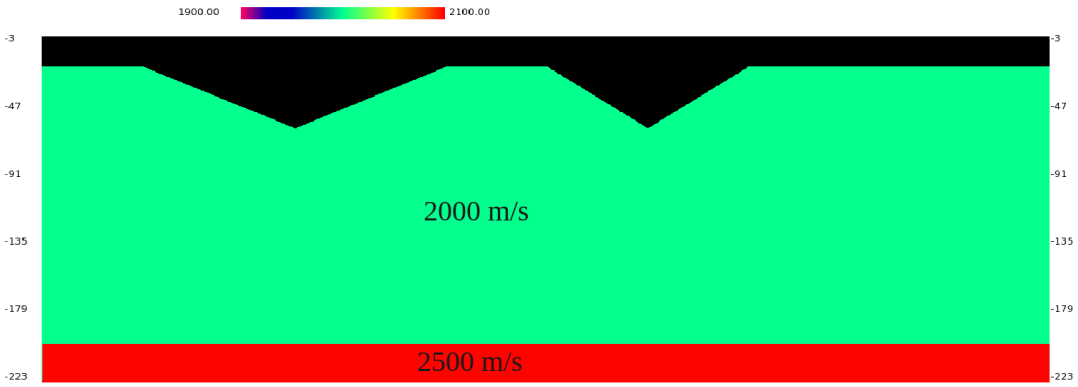

FIG. 8. Near surface velocity model

Two weathering pockets in the model were centred at station 251 and 601. Figure 9 shows synthetic shot record at station 500 with first arrival times overlay. Effects of the low velocity layer can be seen on both sides of the shot point on the deeper reflection events.

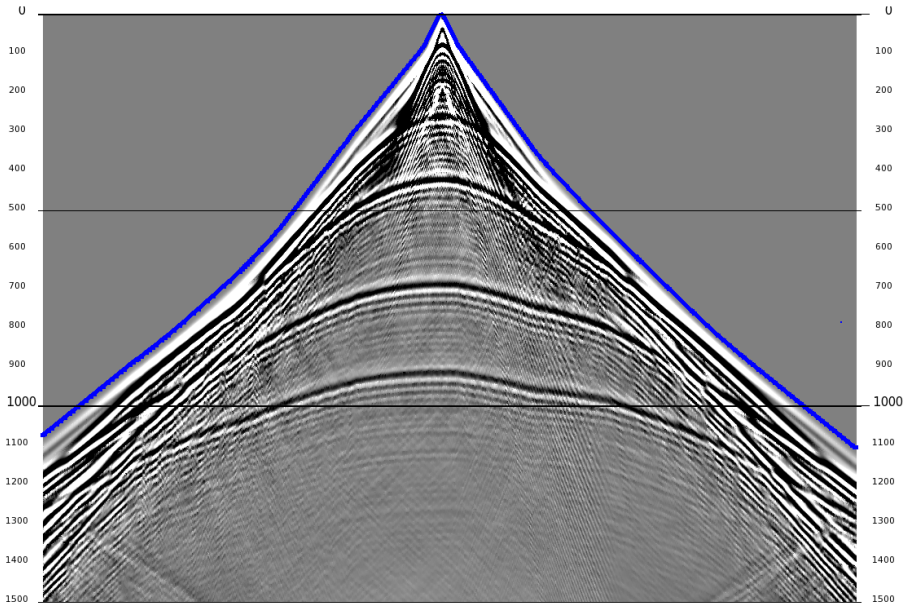

FIG. 9. Shot Point 500

Estimating initial velocity model for GLI analysis

Initial velocity model for GLI analysis can be determined by measuring the slopes and intercept times on a time vs offset (TX) plot. This can also be done by applying linear

moveout (deskewing) with a guess velocity until the first arrival times for the selected layer are flat.

GLI analysis result

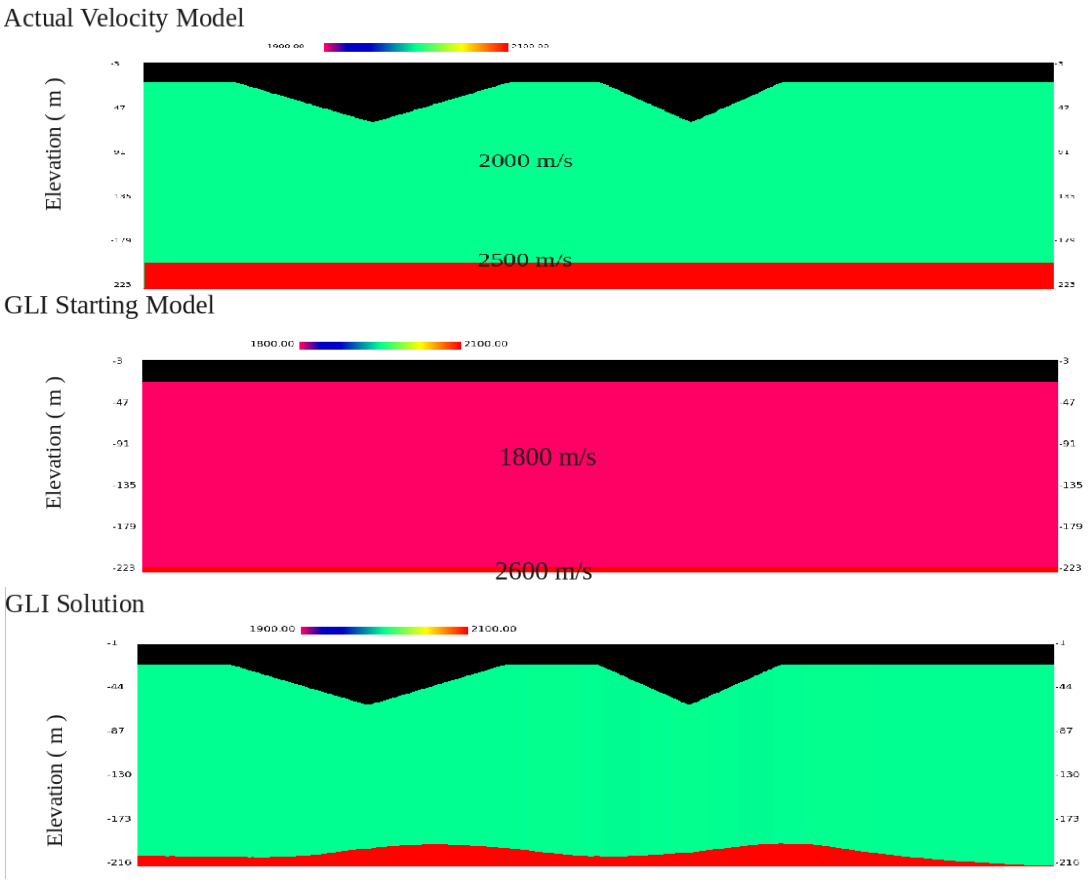

FIG. 10. GLI model and solution

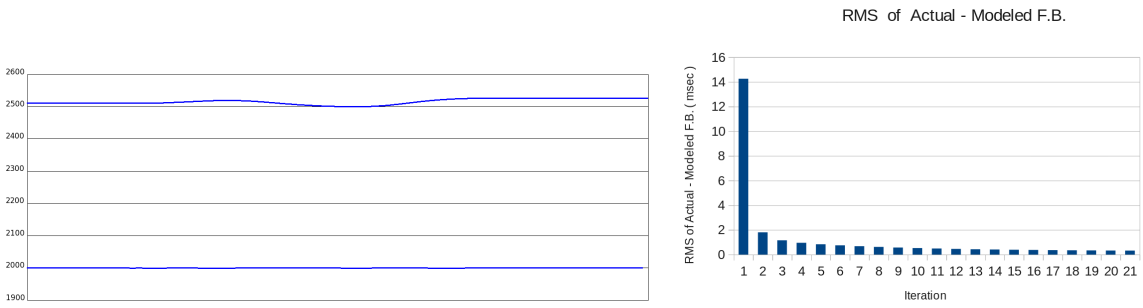

FIG. 11. Velocity solution and RMS of residual error

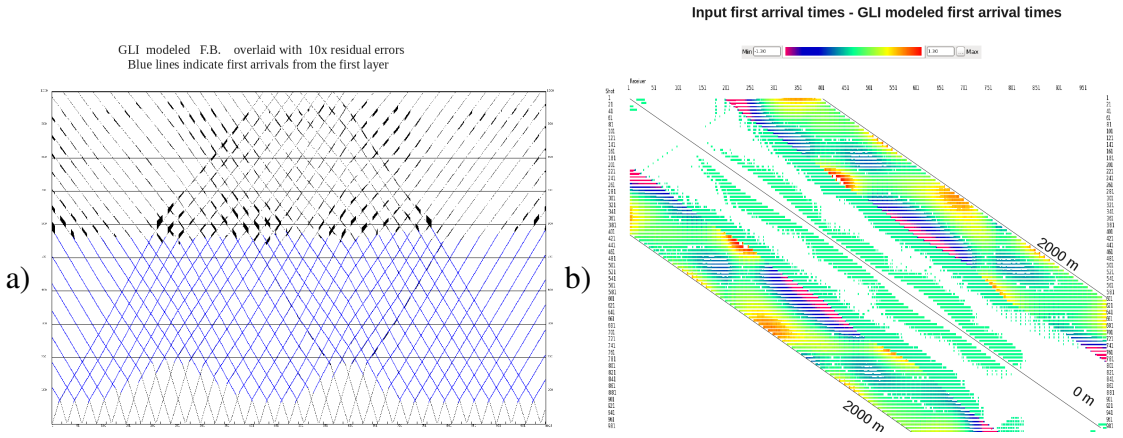

FIG. 12. a) GLI Modeled first arrivals and 10 x residual errors b) surface-consistent display of residual errors

Figure 10 shows the velocity model for the synthetic dataset, the starting model for GLI inversion and the GLI solution. To test the sensitivities of the starting model for GLI inversion, velocities different than the actual model were used in the initial model. Velocity and thickness solution for the first layer almost match the actual model. However, small errors in the first layers are accumulated in the second layer. Because of the higher velocity in the second layer, the magnitude of velocity and thickness errors becomes more apparent. RMS of residual errors after 20 iterations is 0.32 msec (Figure 11).

Figure 12a displays the modeled first arrivals and the residual errors. Residual errors are displayed with 10 times vertical exaggeration and only every 3 shot points are plotted. Figure 12b shows the residual errors in a surface consistent manner with receiver stations along the horizontal axis and shot stations along the vertical axis. There are only a few residual errors greater than 1 msec. and most of the larger residual errors appear at the cross-over points between the first and second layer arrivals as shown in figure 12a. This test demonstrates that the GLI algorithm is capable of modeling near surface velocity changes that follow the layered model assumption and that potential problems can be expected at survey edges where refraction coverage is poor.

Application of GLI solution

GLI solution is used to compute the weathering static corrections using weathering velocity of 1000 m/s and replacement velocity of 2500 m/sec. CDP stacks are created with and without GLI weathering statics. Although the velocity of the GLI solution does not match the actual model at the survey edges, the GLI weathering static corrected the near-surface weathering effects.

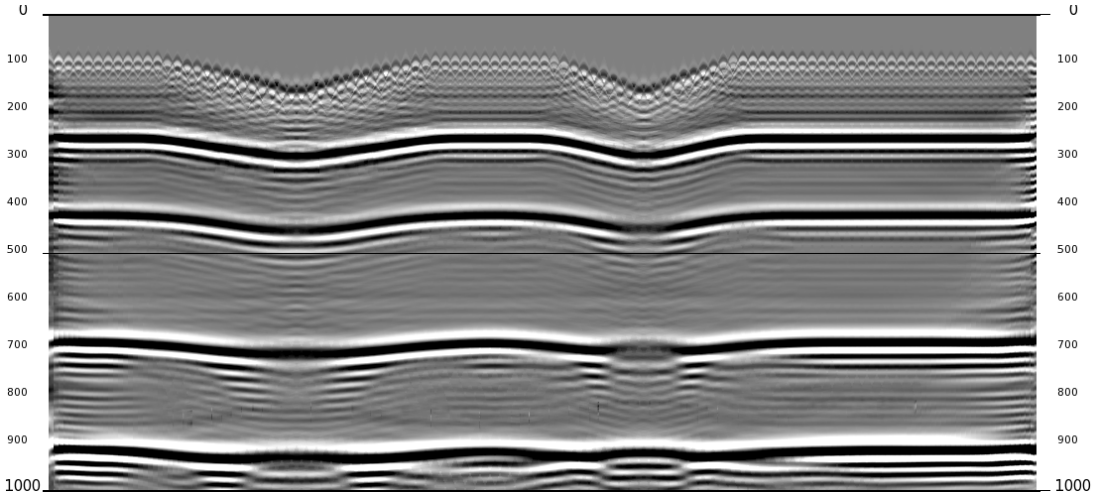

FIG. 13. CDP stack without GLI statics correction

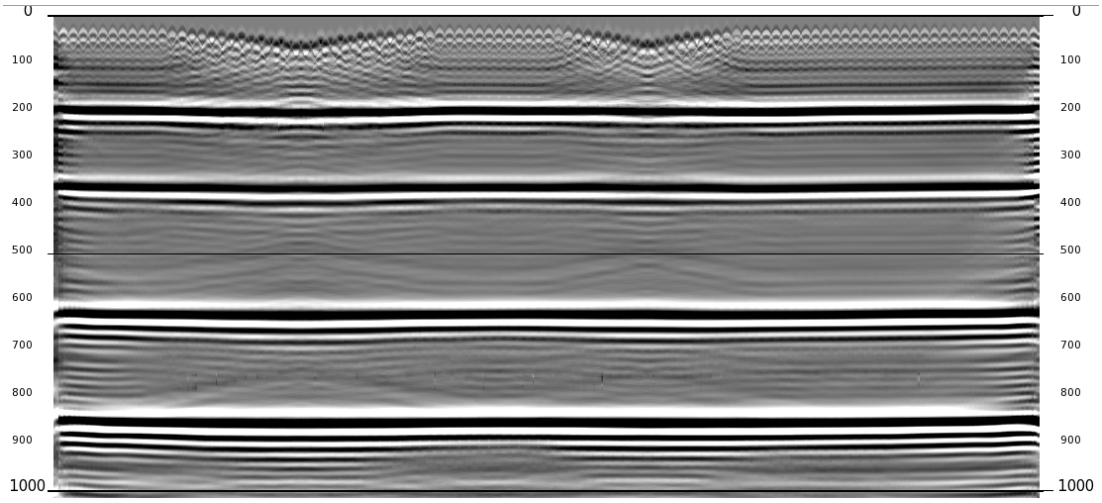

FIG. 14. CDP stack with GLI static correction

Wm test

To verify that model errors can be corrected using surface consistent residual statics computed from reflection data we introduced an anomaly to the GLI solution to create errors in weathering statics correction as shown in figure 15 .

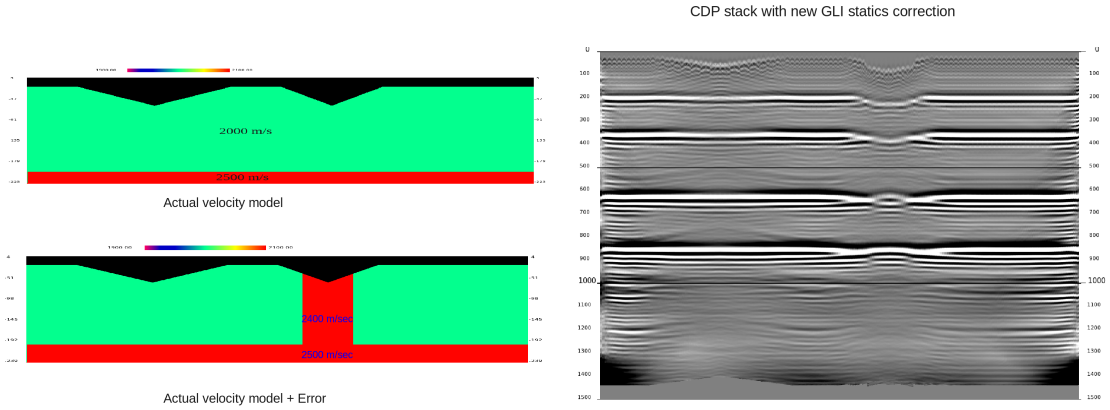

FIG. 15. Input to residual statics and Wm test

Residual statics were computed using stack-power maximization algorithm. Figure 16 shows the residual statics computed and the CDP stack after the application of the residual statics. Figure 17 shows the computed Wm and the corrected velocity model. This test demonstrates the effectiveness of stack-power maximization for residual statics computation and Wm for velocity model correction.

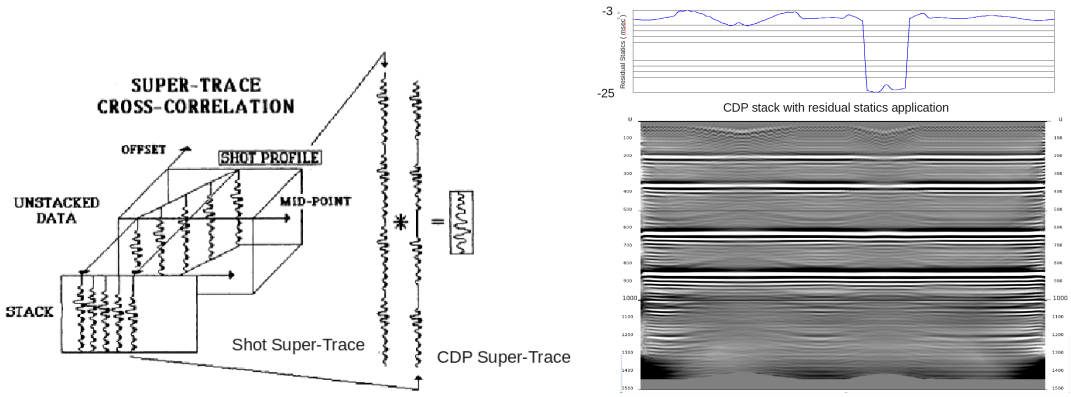

FIG. 16. Residual statics by stack-power maximization(Ronen and Claerbout 1985)

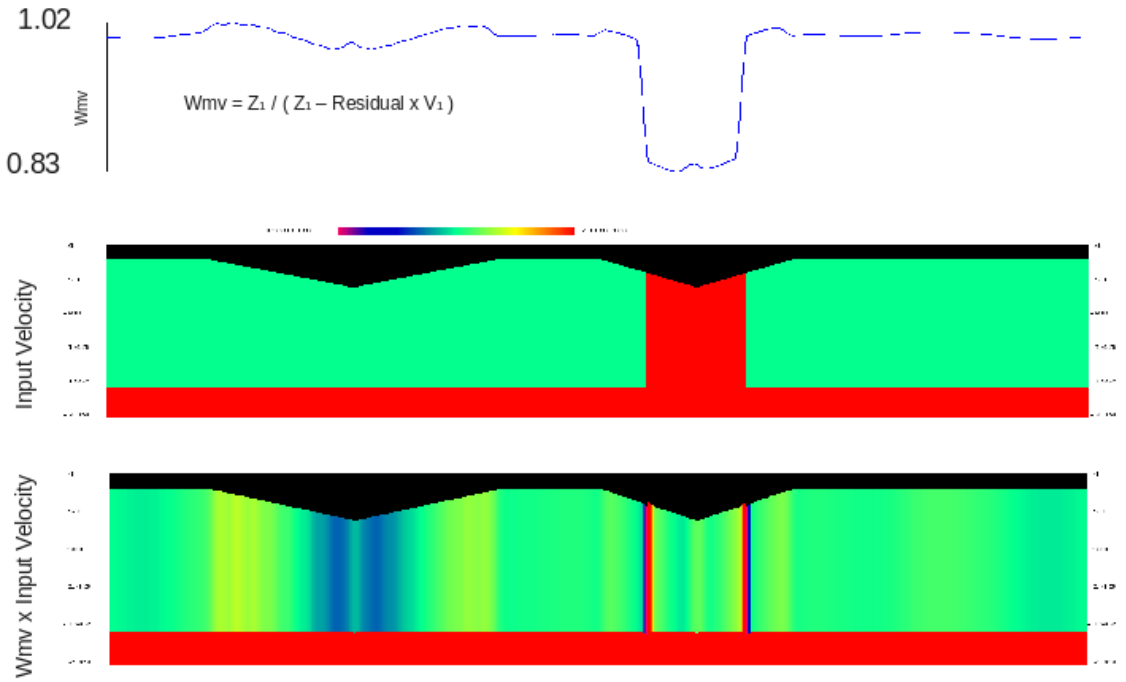

FIG. 17. Wm computation and application

GLI Refraction Analysis of 1994 BP statics benchmark model

The BP statics benchmark model (figure 18) and synthetic dataset were created at the Amoco Tulsa Research Lab in 1994 by Mike O'Brien to evaluate refraction statics algorithms for near surface velocity anomalies and is available as open data. Figure 19 shows the near surface velocity model.

Figure 20 shows a one layer GLI solution with constant weathering velocity of 800 m/s. Figure 21 and 22 compare the CDP stack with datum statics correction only with GLI statics corrected stack. CDP stack with GLI statics correction shows significant improvement. Comparing the GLI solution and the GLI stack to the actual model, we believe that more improvement should be possible. However, extending the GLI solution to 2 layers resulted in an unstable solution and residual statics computed from stack power maximization were small; therefore, they were not used to compute model and data weights for the modified GLI algorithm. Examining the input data to stack-power maximization revealed that we require further processing to improve the data coherence within CDP gathers. Figure 23 shows some example of the input data.

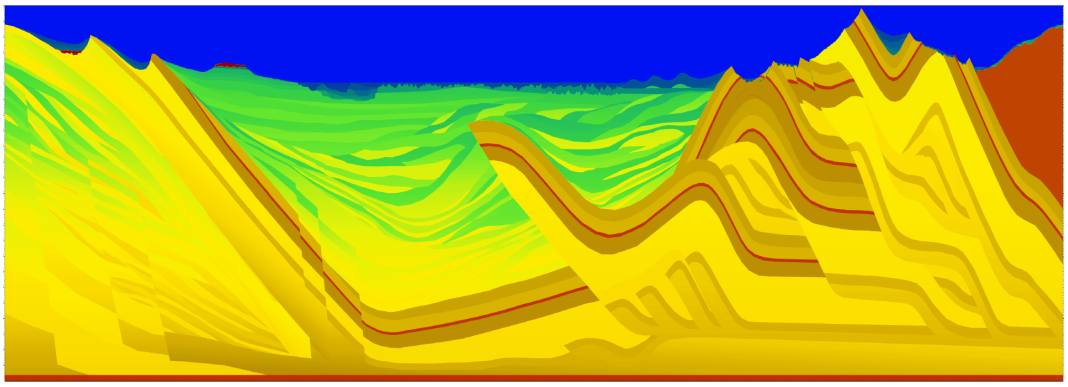

FIG. 18. 1994 BP statics benchmark model

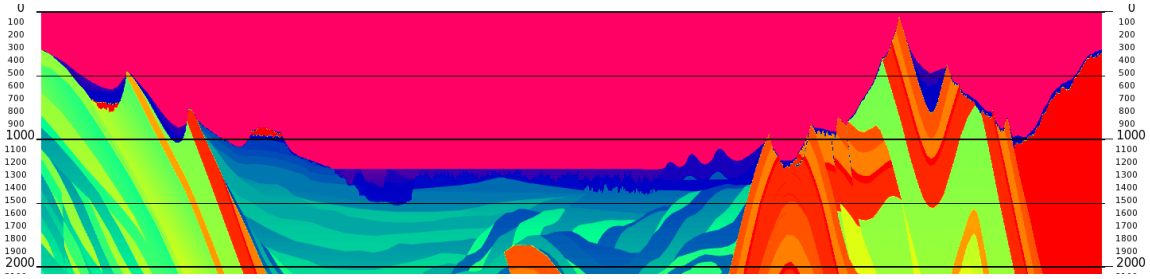

FIG. 19. Near surface velocity

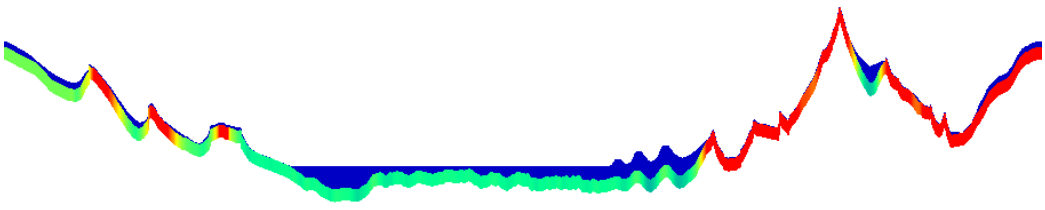

FIG. 20. Velocity from GLI solution

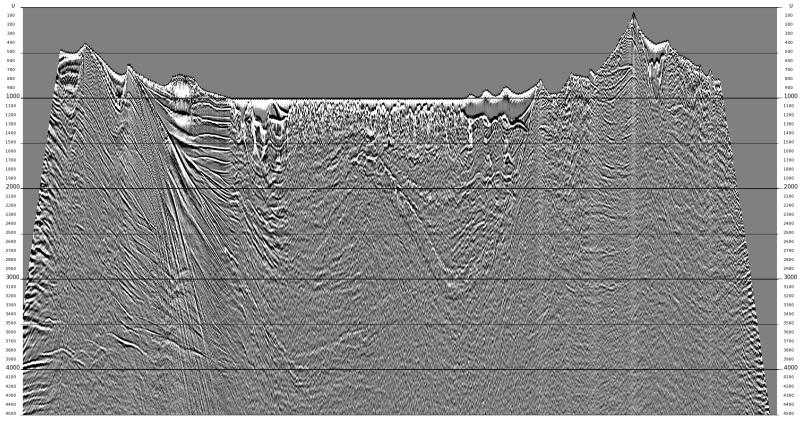

FIG. 21. CDP stack with datum correction

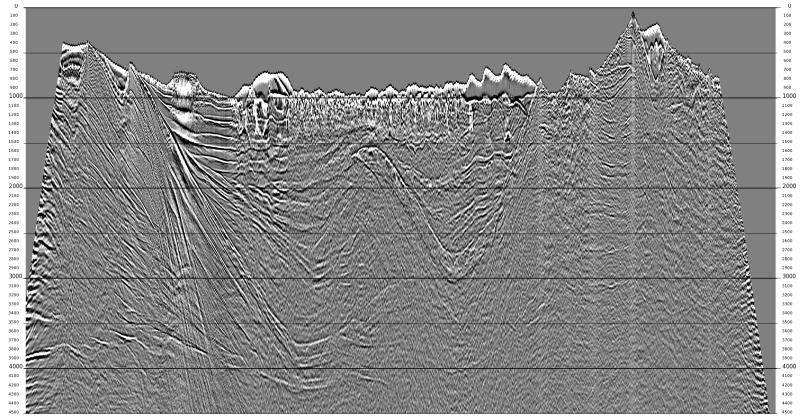

FIG. 22. CDP stack with GLI statics correction

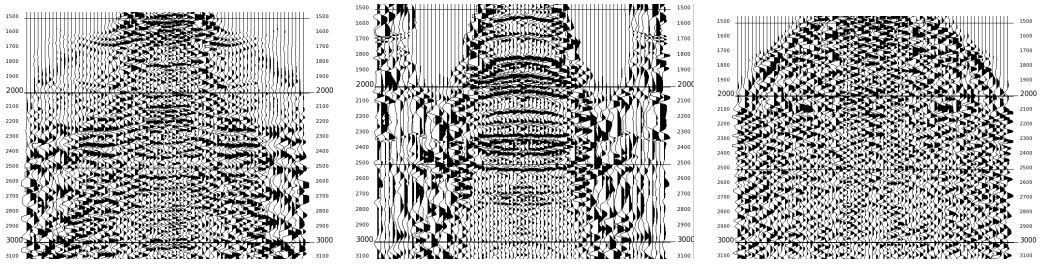

FIG. 23. CDP gather 6000, 8100 and 17000

GLI Refraction Analysis of Spring Coulee 2D-3C P-wave Data

Spring Coulee seismic line 2008-SC-01 starts at station 101 at the north to station 752 at the south and consists of data acquired with Vibroseis and dynamite sources. Vibroseis sources cover shot stations 103 to 689 with a shot point gap between station 160 and 210. Two Mertz buggy mount vibrators were used. Linear sweep of 4-130 Hz was used. The sweep length is 12 second and listening time is 6 seconds. Dynamite sources cover shot stations 266 to 419 and a shot with 2 kg dynamite at 18 m depth is fired every third station.

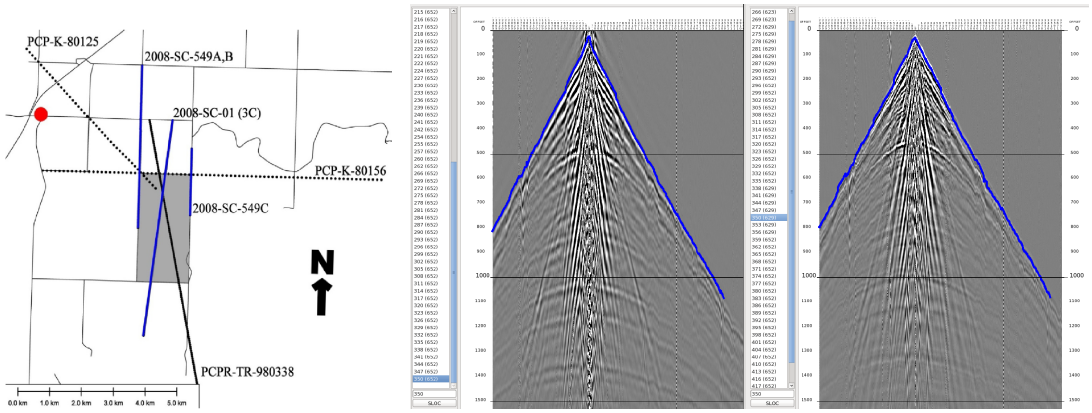

FIG. 24. Vibroseis and dynamite records with first arrival time picks

First arrival times are picked automatically using amplitude criteria and bad picks are edited manually. Initial refraction velocities and intercept times are estimated by applying linear moveout to first arrival time picks with guess velocities. To impose data limitation on the solution, we decimated the data by 75% using only every 4th shot point for the GLI algorithm. Figure 25 shows the velocity model from the GLI algorithm.

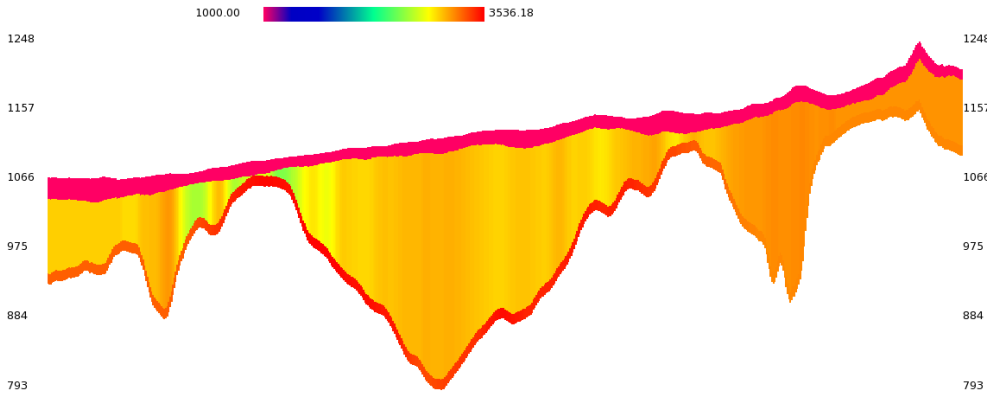

FIG. 25. Velocity from GLI solution

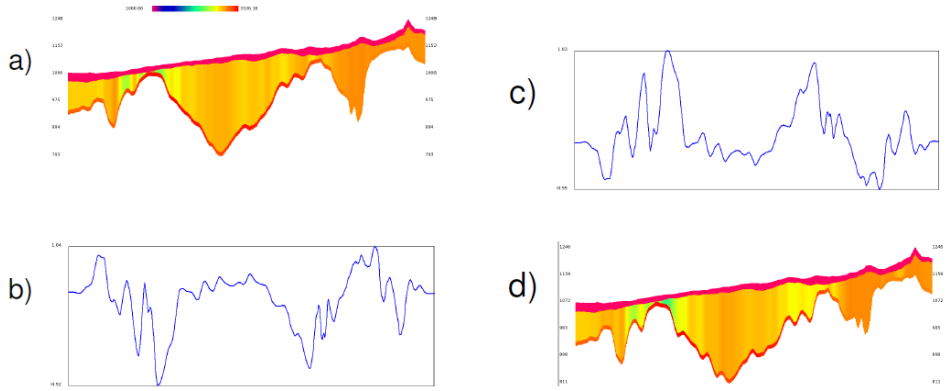

FIG. 26. a) Velocity from GLI solution (CDP 202-1304) b)W_{mv} (0.92-1.04) c) W_{mz} (0.99-1.03) d) GLI solution with W_{mv} and W_{mz} update

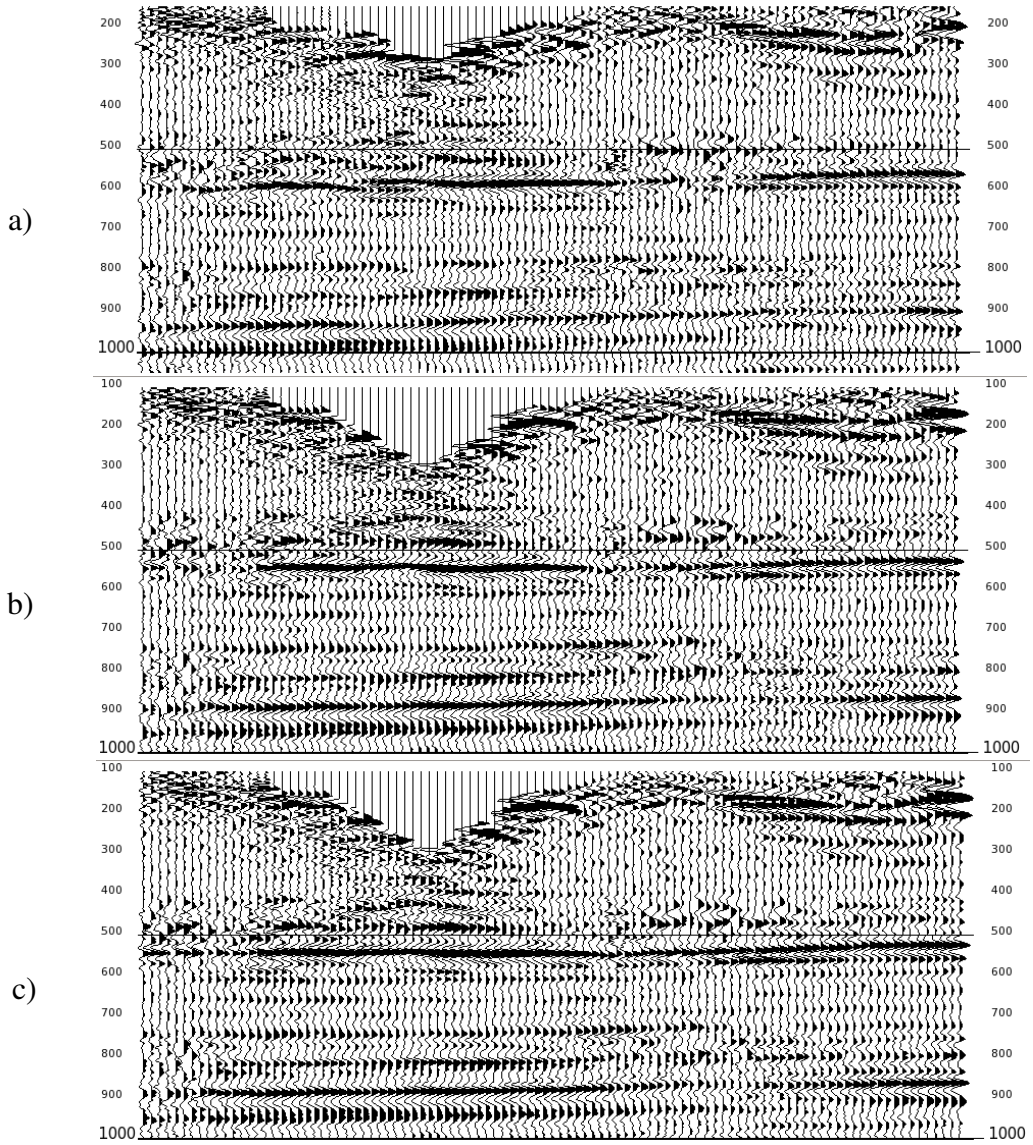

FIG. 27. a) datum statics corrected CDP stack (CDP 300-500) b) GLI statics corrected stack, c) CDP stack with stack-power maximization and GLI solution with W_m update

GLI statics corrected data is used to compute surface-consistent residual statics using stack-power maximization algorithm. The modified GLI algorithm uses the long wavelength component of the surface consistent residual statics to compute model weights W_m and data weights W_d and iteratively updates the near surface velocity model. The final stack is created using short wavelength component of the surface consistent residual statics and the updated GLI solution. Figure 26 shows the model weight, data weight and updated GLI model. Figure 27 compares the elevation stack, GLI corrected stack and the stack from this new approach.

CONCLUSIONS

A non-linear optimization technique for near surface refraction inversion is demonstrated using a synthetic dataset and the Spring Coulee 2D P-P data. All tests done in this report use GLI for refraction analysis and stack-power maximization for reflection residual statics. However, this technique will also work for refraction tomography or other model based refraction method, as well as other reflection residual statics algorithms. Result of the Spring Coulee 2D test using decimated input suggests this approach should work well with 3D surveys and further tests using 3D datasets should be done. Test result for BP94 statics benchmark model revealed that further enhancement to the input data is required prior to surface-consistent residual statics and that refraction tomography is better suited for complex near surface geology.

ACKNOWLEDGMENTS

We thank the sponsors of CREWES and NSERC (Natural Science and Engineering Research Council of Canada) through the grant CRDPJ 461179-13 for supporting this project.

REFERENCES

Al-Saad R. and Bridle R.,2016, Near surface modeling challenges highlighted at SEG/DGS Near-Surface Modeling Workshop, The Leading Edge, 35,620-621

Claerbout,J., 1992,Earth Sounding Analysis:Processing versus Inversion: Standford University

Eaton,D., Cary,P. And Schafer,A., 1991, Estimation of P-SV residual statics by stack-power optimization: https://www.crews.org/ForOurSponsors/ResearchReports/1991/1991-07.pdf

Hampson, D., and Russell, B., 1984, First Break Interpretation using generalized linear inversion:Journal of the Canadian Society of Exploration Geophysicists, 20, 40-54

Henley, D.,2012, Interferometric application of static corrections: Geophysics, 77, Q1-Q13

Lines, L. R., Schultz, A.K and Treitel, S., 1988, Cooperative Inversions of geophysical data: Geophysics, 53,8-20

Lines, L. R., and Treitel, S., 1984, A review of least-squares inversion and its application to geophysical problems: Geophysical Prospecting 32, 159-186

Ronen,J. And Claerbout,J., 1985, Surface-consistent residual statics estimation by stack-power maximization:Geophysics,50, 2759-2767

Schneider,W.,Ranzinger,K.,Balch,A.,Kruse C., 1992, A dynamic programming approach to first arrival traveltime computation in media with arbitrarily distributed velocities: Geophysics 57,39-50

Taner,M., Koehler,F., and Alhilali,K.,1974,Estimation and correction of near-surface time anomalies: Geophysics,39,441-463

Trad,D.,Ulrych,T.,Sacchi,M.,2003,Latest views of the sparse Radon transform:SEG Technical Program Expanded Abstracts, 1929-1932.

Won, J. and Bevis, M., 1984, The hidden-layer problem revisited: Geophysics, 49, 2053-2056

Zhou,H., Gray, S., Young, J., Pham, D., Zhang, Y., 2002, Tomographic Residual Curvature Analysis:The Process and its Components:SEG Technical Program Expanded Abstracts,666-669.